Forest Chemicals Revew
www.forestchemicalsreview.com
ISSN: 1520-0191
July-August 2021 Page No. 1662-1670
Article History: Received: 12 May 2021 Revised: 25 June 2021 Accepted: 22 July 2021 Publication: 31 August 2021

Numerical Simulation of Flow Field and Rigidity Analysis for Runner Blade of Francis Turbine

Zhihua Yao*, Shaoling Li, Yuren Zhang
College of Mechanical Engineering, Anhui Science and Technology University, Fengyang, Anhui, China
*Corresponding Author.

Abstract:

A self-designed HL200-LJ-200 Francis turbine was numerically simulated based on computational fluid dynamics to study the characteristics of internal flow field within it. Based on the pressure distribution of runner blade obtained by numerical simulation, the rigidity and strength of runner blade were analyzed by finite element method. The results showed the pressure variation of Francis turbine was concentrated in the area of the runner, the pressure of the volute inlet was the highest and the center of runner was the lowest, the maximum velocity in the flow field was mainly on the center of runner blade, and the average pressure and velocity increased as the volume flow rate increased. The turbulent kinetic energy and the vorticity of Francis turbine were both mainly distributed in the runner blade and stern pipe elbow area. The runner blade met the requirements of rigidity and strength. The results provided a theoretical basis for improving the performance and reliability of Francis turbines.

Keywords*: Francis turbines, Numerical simulation, Internal flow, Rigidity and strength analysis.*

I. INTRODUCTION

Because of their flexible output power, hydraulic turbines have been widely used to match the generation of energy, the performance of hydraulic turbines directly determines efficiency and economic benefit of the power generation. The most common type was the Francis turbine due to its versatility in terms of design head [1-4]. Conventional turbine design was based on design experience and lacks effective mechanism analysis. However, it was very difficult to calculate the internal flow field because of the complicated structure and irregular geometrical surface of Francis turbine. However, experimental research was usually expensive, and it is

Forest Chemicals Revew
www.forestchemicalsreview.com
ISSN: 1520-0191
July-August 2021 Page No. 1662-1670
Article History: Received: 12 May 2021 Revised: 25 June 2021 Accepted: 22 July 2021 Publication: 31 August 2021

difficult to simulate high-speed flow problems by experimental means, so experimental research was also limited [5]. Computational fluid dynamics (CFD) can effectively simulate complex flow fields and has become an important method to study the flow field of Francis turbines [6-10]. In this paper, based on CFD and finite element method (FEM), numerical simulation and analysis of flow field characteristics and rigidity and strength of runner blade of Francis turbine were studied. The research results can provide theoretical reference for design and performance improvement of Francis turbines.

II. BASIC EQUATIONS

2.1 Numerical Models

The flow inside the Francis turbine belonged to three-dimensional unsteady flow. Assuming that the flow was isothermal, the basic numerical models could be described as follows.

Continuity equation could be expressed by Eq. (1).

$$\frac{\partial \rho}{\partial t} + \frac{\partial (\rho u_i)}{\partial x_i} = 0 \tag{1}$$

Where ρ was the density of mixture flow, u_i represented average velocity, t was the time.

Momentum equation was described by Eq. (2).

$$\frac{\partial (\rho u_i)}{\partial t} + \frac{\partial (\rho u_i u_j)}{\partial x_j} = -\frac{\partial p}{\partial x_i} + \frac{\partial \tau_{ij}}{\partial x_j} \tag{2}$$

Where u_i and u_j represented average velocity, p denoted static pressure of mixture flow, τ_{ij} denoted the stress tensor, which could be expressed by Eq. (3).

$$\tau_{ij} = (\mu + \mu_t)\left\{\frac{\partial u_i}{\partial x_j} + \frac{\partial u_j}{\partial x_i}\right\} \tag{3}$$

Forest Chemicals Revew
www.forestchemicalsreview.com
ISSN: 1520-0191
July-August 2021 Page No. 1662-1670
Article History: Received: 12 May 2021 Revised: 25 June 2021 Accepted: 22 July 2021 Publication: 31 August 2021

Where μ_t was the turbulence viscosity.

2.2 Turbulence Model

RNG $k-\varepsilon$ model was used for turbulence model, which could be expressed by Eq. (4) and Eq. (5).

$$\frac{\partial(\rho k)}{\partial t}+\frac{\partial(\rho k u_i)}{\partial x_i}=\frac{\partial}{\partial x_i}\left[\left(\mu+\frac{\mu_i}{\sigma_k}\right)\frac{\partial k}{\partial x_i}\right]+G_k-\rho\varepsilon \quad (4)$$

$$\frac{\partial(\rho\varepsilon)}{\partial t}+\frac{\partial(\rho\varepsilon u_i)}{\partial x_i}=\frac{\partial}{\partial x_i}\left(\alpha_\varepsilon\mu_{eff}\frac{\partial\varepsilon}{\partial x_i}\right)+C_{\varepsilon1}\frac{\varepsilon}{k}G_k+C_{\varepsilon2}\frac{\varepsilon^2}{k}-R \quad (5)$$

Where k was turbulent kinetic energy, e represented turbulent dissipation rate, G_k was generation term and μ_{eff} was Effective viscosity coefficient.

2.3 Design and Modeling of Francis Turbine

TABLE I. Parameters of Francis turbine

PARAMETERS	**VALUE**
water head/*m*	100
volume flow rate/ m^3s^{-1}	38
diameter of runner/*mm*	2000
Number of runner blades	16
Inlet diameter of volute/*mm*	2500

In this design, the type of Francis turbine was HL200-LJ-200. According to the parameters shown in Table I, the main components of the Francis turbine such as runner, runner blade, spindle and volute were designed. Three dimensional(3D) modeling was carried out using SolidWorks 2014 software. The 3D geometric model of the Francis turbine was shown in Fig 1, the runner and runner blade were shown in Fig 2.

Forest Chemicals Revew
www.forestchemicalsreview.com
ISSN: 1520-0191
July-August 2021 Page No. 1662-1670
Article History: Received: 12 May 2021 Revised: 25 June 2021 Accepted: 22 July 2021 Publication: 31 August 2021

Fig 1: Three dimensional geometric model

Fig 2: Runner and runner blade

2.4 Grid Division and Boundary Condition

The calculation area and grid division were shown in Fig 3, and the number of grids was 2658392.

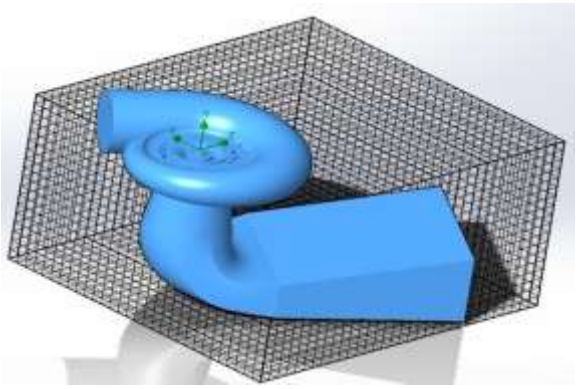

Fig 3: Calculation area and grid division

SIMPLE algorithm was used to solve the time-mean N-S equation of incompressible fluid. The inlet of the turbine volute was set as volume flow rate, the outlet of the tailpipe was set as pressure outlet boundary condition, and the wall was set as no slip boundary condition. Gravity acceleration -9.81m/s^2 was applied to the water body in the Y direction.

Forest Chemicals Revew
www.forestchemicalsreview.com
ISSN: 1520-0191
July-August 2021 Page No. 1662-1670
Article History: Received: 12 May 2021 Revised: 25 June 2021 Accepted: 22 July 2021 Publication: 31 August 2021

III. ANALYSIS OF SIMULATION RESULTS

3.1 Analysis of Flow Field

3.1.1 Flow field distribution

Fig 4 to Fig 7 showed the distribution of pressure, velocity, turbulent kinetic energy and vorticity under design conditions, in which the volume flow rate Q was $38m^3/s$ and the outlet pressure was a standard atmospheric pressure.

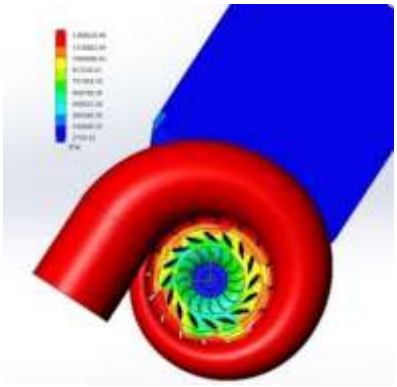

Fig 4: Pressure distribution

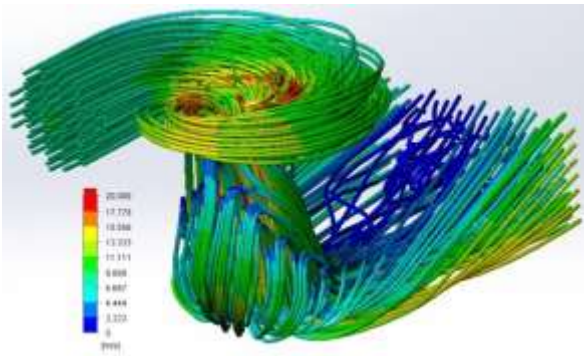

Fig 5: Velocity distribution

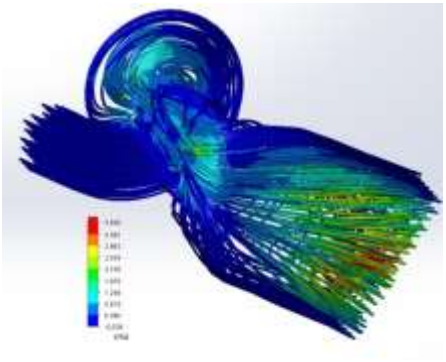

Fig 6: Turbulent kinetic energy distribution

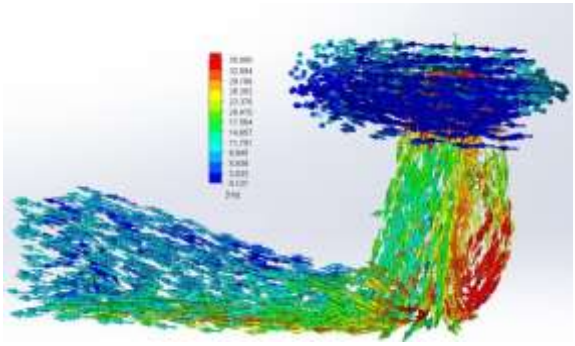

Fig 7: Vorticity distribution

It can be seen from Fig 4 that the pressure variation of Francis turbine was concentrated in the area of the runner blade, the pressure of the volute inlet was the highest and the center of runner was the lowest. As can be seen from Fig 5, the maximum velocity in the flow field was mainly on the center of runner, the sudden decrease of the volume area of the runner area led to the increase of flow velocity. The flow velocity in the middle of the tailpipe was low and even

Forest Chemicals Revew
www.forestchemicalsreview.com
ISSN: 1520-0191
July-August 2021 Page No. 1662-1670
Article History: Received: 12 May 2021 Revised: 25 June 2021 Accepted: 22 July 2021 Publication: 31 August 2021

backflow occurs, which was caused by the negative pressure generated during the operation of Francis turbine. As shown in Fig 6, the turbulent kinetic energy was mainly distributed in the runner blade area, the stern pipe elbow part and the stern pipe outlet. As shown in Fig 7, the vorticity of Francis turbine was mainly concentrated in the runner blade and the tailpipe elbow, which is caused by the rotation of the runner blade and the special structure of turbine.

3.1.2 Pressure and velocity distribution under different volume flow rate

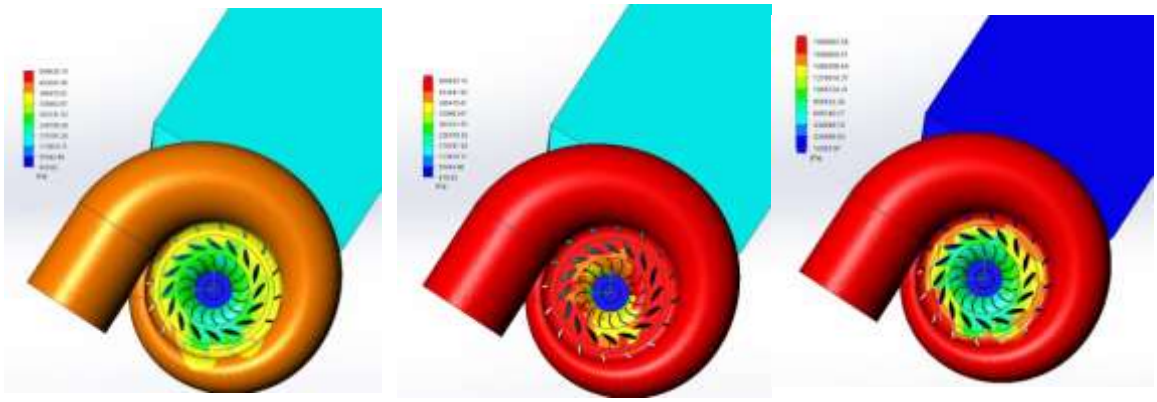

(a) (b) (c)

Fig 8: Pressure distribution in Francis turbine under different volume flow rate

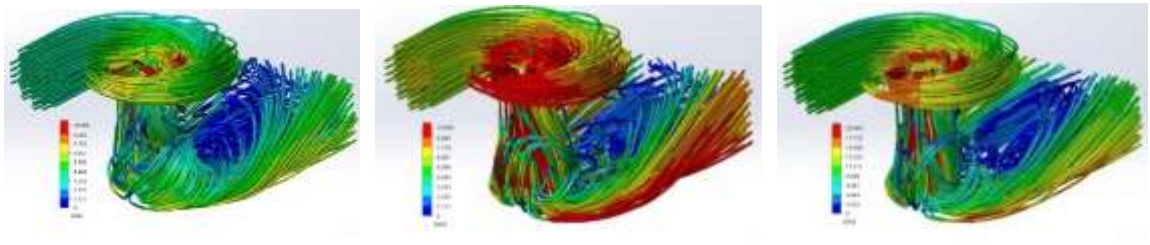

(a) (b) (c)

Fig 9: Velocity distribution in Francis turbine under different volume flow rate

TABLE II. Average pressure and velocity under different volume flow rate

Flow Field features	0.5Q	0.8Q	1Q	1.2Q
Average pressure/*Pa*	208546	337127	4576675	597896
Average velocity/ ms^{-1}	4.07	6.20	7.80	9.45

Fig 8 and Fig 9 showed the pressure distribution and velocity distribution in the Francis

Forest Chemicals Revew
www.forestchemicalsreview.com
ISSN: 1520-0191
July-August 2021 Page No. 1662-1670
Article History: Received: 12 May 2021 Revised: 25 June 2021 Accepted: 22 July 2021 Publication: 31 August 2021

turbine, in which the outlet pressure was one standard atmosphere and inlet volume flow rates were 0.5Q, 0.8Q and 1.2Q, respectively, where Q was the original design volume flow rate with the number of $38m^3/s$. Table II showed average pressure and velocity under four different inlet volume flow rates. It can be seen that the average pressure and velocity increases as the flow rate increases, the pressure at the center of the runner is the lowest and the velocity is the highest, which was consistent with Bernoulli's equation.

3.2 Analysis of Rigidity and Strength Analysis

Due to mechanical and hydraulic effects, the blade of the Francis turbine was easily damaged due to its thin-walled structure [11]. Therefore, rigidity and strength analysis of runner blade of Francis turbine were needed.

The runner blade density was $7800kg/m^3$, elastic modulus was 2×10^{11}GPa, material yield strength was 248MPa, Poisson's ratio was 0.30, tetrahedral mesh with 28293 nodes were adopted, and full constraints were imposed on the connection between blade and runner. The blade grid model was shown in Fig 10.

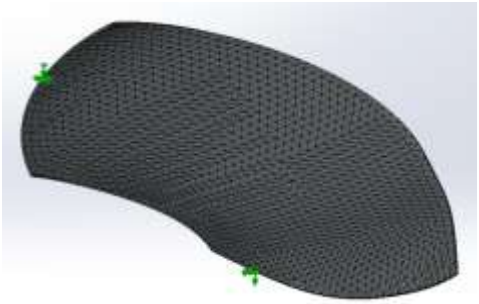

Fig 10: Grid model of runner blade

Under design working conditions, the aforementioned flow field calculation results showed that the average pressure on the face water surface of runner blade was 495760*Pa*, and the average pressure on the back water surface was 390389*Pa*.The pressure was applied to the runner blade to analyze the stress and displacement of the runner blade.

Fig 11 and Fig 12 showed the distribution of stress and displacement of runner blade. As can be seen from Fig 11, the maximum stress of the blade was located at the water edge of the lower ring, and the maximum stress was 11766589Pa, which was smaller than the yield strength of the material of runner blade and met strength requirement. As shown in Fig 12, the maximum displacement of the blade was located at the lower ring, and the maximum

Forest Chemicals Revew
www.forestchemicalsreview.com
ISSN: 1520-0191
July-August 2021 Page No. 1662-1670
Article History: Received: 12 May 2021 Revised: 25 June 2021 Accepted: 22 July 2021 Publication: 31 August 2021

displacement was 0.05mm, which met the rigidity requirement.

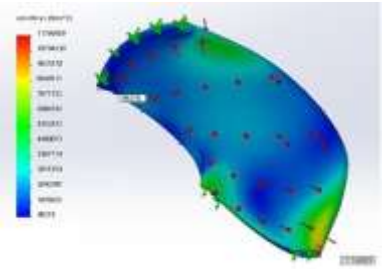

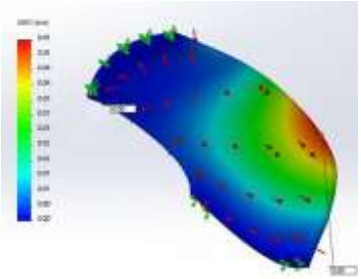

Fig 11: Stress of runner blade Fig12: Displacement of the runner blade

IV. CONCLUSION

In this paper, the internal flow field of HL200-LJ-200 Francis turbine was numerically simulated based on CFD and the rigidity and strength analysis strength of runner blade were analyzed by FEM method. The results showed that the average pressure and velocity increased as the volume flow rate increased, the minimum pressure and the maximum velocity were both located in the area of the center of runner. FEM results showed that the runner blade met the requirements of rigidity and strength. The results provided a theoretical basis for improving the performance and reliability of Francis turbines.

ACKNOWLEDGEMENTS

This research were supported by Natural Science Research Project of Higher Education of Anhui Province (Grant No. KJ2019A0808) and Central Guide Local Science and Technology Development Special Project of Anhui Province (Grant No. 202007d08050022).

REFERENCES

[1] Zhao WQ, Presas A, Egusquiza M, et al. (2021) Increasing the operating range and energy production in Francis turbines by an early detection of the overload instability. Measurement 181: 1-11

[2] Li ZC, Chang JS, Xin Z (2013) Numerical simulation of elimination of pressure fluctuation in Francis turbine draft tube using water jet. Transactions of the Chinese Society for Agricultural Machinery 44(1): 53-57

Forest Chemicals Revew
www.forestchemicalsreview.com
ISSN: 1520-0191
July-August 2021 Page No. 1662-1670
Article History: Received: 12 May 2021 Revised: 25 June 2021 Accepted: 22 July 2021 Publication: 31 August 2021

[3] Mauro S, Lanzafame R, Brusca S (2019) Unsteady computational fluid dynamics analysis of the hydrodynamic instabilities in a reversible Francis turbine used in a storage plant. Heliyon 5: 1-15

[4] Vytvytskyi L, Lie B (2018) Mechanistic model for Francis turbines in Open Modelica. IFAC PapersOnline 51(2): 103-108

[5] Unterluggauer J, Sulzgruber V, Doujak E (2020) Experimental and numerical study of a prototype Francis turbine startup, Renew. Energy 157: 1212-1221

[6] Huang JF, Zhang LX, Wang WQ, et al. (2010) Numerical simulation of turbulent flow in vane passage based on dynamical mesh technology. Journal of Drainage and Irrigation Machinery Engineering 28(2): 140-143

[7] Li M, Xiao JL, Wang G, et al. (2012) Three-dimensional unsteady numerical simulation of ring gate emergency shut-down for hydraulic turbine. Journal of Hydroelectric Engineering 31(2): 228-234

[8] Kang MW, Park N, Suh SH (2016) Numerical study on sediment erosion of Francis turbine with different operating conditions and sediment inflow rates. Procedia Engineering 157: 457-464

[9] Valerii P, Alexandr Z, Salienko E (2017) Numerical and experimental research of natural frequencies and mode shapes for runner of Francis turbine. Procedia structures integrity 6: 224-227

[10] Choi HJ, Zullah MA, Roh HW, et al. (2013) CFD validation of performance improvement of a 500 kW Francis turbine. Renewable Energy 54: 111-123

[11] Müller A, Favrel A, Landry C, et al. (2017) Fluid–structure interaction mechanisms leading to dangerous power swings in Francis turbines at full load. J. Fluids Struct 69: 56-71